

# Text-Guided Layer Fusion Mitigates Hallucination in Multimodal LLMs

Chenchen Lin<sup>1</sup>, Sanbao Su<sup>1</sup>, Rachel Luo<sup>2</sup>, Yuxiao Chen<sup>2</sup>,  
Yan Wang<sup>2</sup>, Marco Pavone<sup>2,3</sup>, Fei Miao<sup>1</sup>

<sup>1</sup>University of Connecticut    <sup>2</sup>NVIDIA    <sup>3</sup>Stanford University  
{chenchen.lin, sanbao.su, fei.miao}@uconn.edu  
{raluo, yuxiaoc, yanwan, mpavone}@nvidia.com

## Abstract

Multimodal large language models (MLLMs) often generate confident but visually ungrounded responses, a phenomenon known as hallucination. While prior mitigation methods primarily operate at decoding time or rely on additional training, they typically expose the language model to a fixed, late-layer visual representation, overlooking the rich hierarchy encoded by vision transformers. We show that hallucination behavior is strongly influenced by the depth of visual features provided to the LLM, and that no single layer is optimal across queries. To address this, we propose Text-Guided Inter-layer Fusion (TGIF), a lightweight architectural module that dynamically reweights visual features across transformer layers based on the input text, without modifying the vision encoder or increasing the token budget. Experiments on hallucination, OCR, and general VQA benchmarks demonstrate that TGIF substantially improves visual grounding and hallucination robustness while preserving strong overall reasoning performance.

## 1 Introduction

Multimodal large language models (MLLMs) combine the reasoning capabilities of large language models (LLMs) with pre-trained vision encoders, achieving impressive results in diverse visual tasks [26, 18, 9]. However, MLLMs face persistent hallucination challenge, generating confident but ungrounded content that is plausible under language priors yet inconsistent with the image [24]. This is particularly pronounced in detail-oriented tasks where high-level semantic features alone are insufficient for precise grounding. Most existing hallucination mitigation methods intervene after training or at inference time [13, 46, 16, 27, 14, 36, 6]. While effective, these approaches primarily operate on the text generation process and leave the underlying visual representations unchanged.

A key but underexplored factor is the depth of visual representations exposed to the language model. Vision transformers such as CLIP encode a hierarchy of visual abstractions across

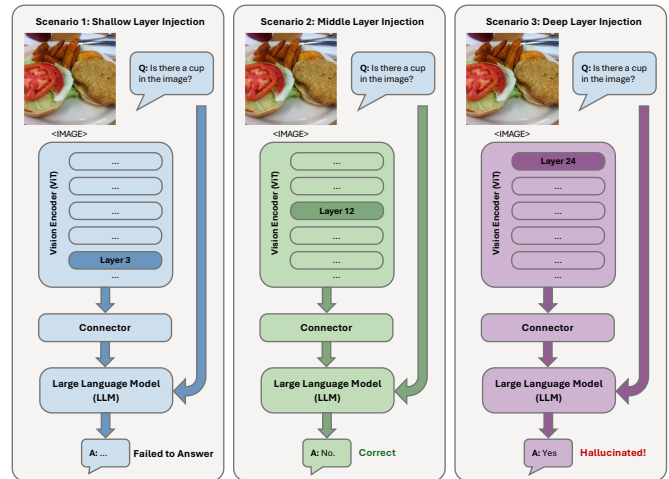


Figure 1: **Impact of ViT Layer Injection on Hallucination Behavior.** The figure illustrates three scenarios: (1) Shallow layer injection leads to a lack of semantic understanding. (2) Middle layer injection captures sufficient object-level features for an accurate answer. (3) Deep layer injection can lead to hallucination or misinterpretation of the global context.

layers, ranging from low-level spatial cues to high-level semantic concepts. However, most MLLMs expose only a single, fixed (typically late) vision layer to the LLM via an MLP projector. Figure 1 presents a representative example in which the baseline LLaVA model hallucinates, demonstrating that injecting visual features from different depths, with all other components held fixed, results in qualitatively different behaviors ranging from under-recognition to hallucination.

Recent works begin to highlight the role of visual encoder layers in MLLMs, suggesting that shallow and middle layers exhibit unique strengths over deep layers in certain sub-tasks [7]. VaLiD [27] and LayerCD [6] collectively suggest that hallucination behavior is sensitive to the choice of visual feature depth. To the best of our knowledge, however, no prior work has addressed this issue by explicitly modifying the multimodal architecture to dynamically control which visual representations are exposed to the LLM.

Motivated by this observation, we hypothesize that hallucination in MLLMs is strongly influenced by how visual features are selected and exposed to the language model, and that

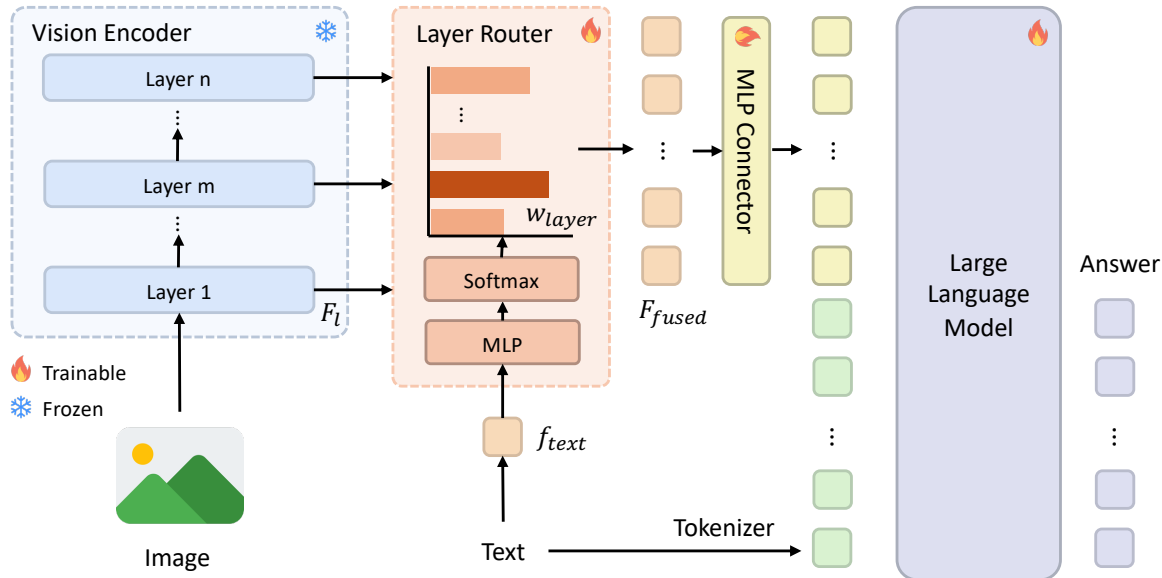


Figure 2: **Overview of the proposed Text-Guided Inter-Layer Fusion (TGIF) framework.** TGIF dynamically integrates hierarchical visual features from a frozen vision encoder based on the textual query. The image is first processed by the Vision Transformer (ViT), producing multi-layer representations  $\{F_l\}$  that capture progressively abstract semantics. The Layer Router receives the text embedding  $f_{text}$  and outputs a soft distribution over encoder layers  $w_{layer}$  through an MLP and softmax. These weights determine the contribution of each layer to the fused visual feature  $F_{fused}$ , which is then projected to the text space by a lightweight MLP connector. The fused multimodal tokens are concatenated with the tokenized text and fed into the LLM for reasoning and response generation.

adapting this selection based on the input prompt can improve visual grounding. We propose **TGIF** (Text-Guided Inter-layer Fusion), a lightweight architectural module that dynamically reweights visual features across all layers of a frozen vision encoder according to the textual query (Fig. 2). This design preserves the pretrained backbone and token budget while enabling prompt-dependent control over visual abstraction.

We instantiate TGIF on top of LLaVA-1.5 and evaluate it on hallucination, OCR, and general VQA benchmarks. TGIF consistently improves hallucination robustness and fine-grained visual perception while maintaining competitive performance on general reasoning tasks, demonstrating that better visual grounding can be achieved through dynamic representation-level control rather than post hoc decoding intervention. Our main contributions are three-fold:

- We identify a limitation of current MLLMs: visual tokens are typically drawn from a single late-layer representation, which is poorly suited for detail-sensitive grounding and exacerbates hallucination under strong language priors.
- We propose **TGIF**, a text-guided inter-layer fusion module that dynamically reweights CLIP layers per query while remaining parameter- and token-efficient. We explore both text-only and multimodal routers and introduce an entropy-based load-balancing loss.
- We show that TGIF improves hallucination robustness and fine-grained visual perception on POPE, Hallusion-

Bench, OCRBench, and TextVQA, while maintaining competitive performance on general reasoning benchmarks.

## 2 Related Work

### 2.1 Multimodal Large Language Models

Multimodal large language models (MLLMs) integrate the reasoning ability of LLMs with the perceptual capacity of pretrained vision encoders. Most follow a modular design with a frozen vision encoder, a lightweight connector, and a powerful LLM decoder. The connector projects visual embeddings into the text space, enabling cross-modal alignment essential for grounded reasoning. Early designs used simple MLP projectors [26], while later approaches like BLIP-2 [18] and InstructBLIP [9] employ query-based modules for salient visual token extraction. Despite architectural differences, a common assumption across these models is that penultimate visual encoder layer is sufficient for all queries.

### 2.2 Hallucination Mitigation in MLLMs

Multimodal large language models (MLLMs) are prone to generating confident yet visually ungrounded responses, commonly referred to as hallucinations [32, 24]. Training-based mitigation approaches typically rely on additional instruction tuning, contrastive fine-tuning, or reinforcement learning from human feedback (RLHF) [13, 46], but introduce substantial

computational and data costs. Training-free methods primarily operate at the decoding stage, for example by calibrating token probabilities, modifying attention patterns, or applying causal masking [16, 27, 14, 36, 6]. While effective in practice, these approaches largely act on the language generation process, without explicitly addressing how visual representations are selected and exposed to the language model.

Recent studies begin to highlight the role of visual representations in hallucination. VaLiD [41] attributes hallucination to distortions in visual encoding and mitigates it via visual layer fusion combined with contrastive decoding guided by uncertainty. LayerCD [39] further demonstrates that hallucinated outputs can be suppressed by contrasting decoding behaviors induced by shallow versus deep visual features. Despite differing hypotheses, these works collectively suggest that hallucination behavior is sensitive to the choice of visual feature depth.

### 2.3 Multi-Layer Visual Feature Fusion

Transformer-based vision encoders like CLIP exhibit a hierarchical structure where deeper layers capture semantic abstraction and intermediate layers preserve fine-grained spatial cues [31, 12]. DenseConnector [42] concatenates features from multiple layers, while MMFuser [5] retrieves shallow-layer details using deep-layer queries. These static strategies enrich representations but cannot adapt fusion to each query. Recent work also systematically analyzes layer integration strategies, showing that direct external fusion yields the most stable performance [21]. Building on these insights, TGIF performs text-guided inter-layer fusion, dynamically reweighting visual features according to the input query to improve grounding and reduce hallucination. Figure 6 in the Appendix provides a schematic comparison between static multi-layer fusion designs and our proposed text-guided routing.

## 3 Method

Our approach is situated within a standard Vision Language Model (VLM) architecture, which comprises a vision encoder (e.g., CLIP ViT [31]), a language model (e.g., Vicuna [8]), and a multimodal projector that maps visual features into the language model’s embedding space. Our proposed text-guided layer selection module is designed as a core component of this multimodal projector. It takes as input the full stack of hidden states from the all vision encoder layers, along with features derived from the text prompt, to produce a dynamically tailored visual representation for the LLM.

### 3.1 Text-Guided Layer Selection

As established in prior work [7], different CLIP layers capture distinct semantic information, with shallow layers encoding textures and spatial details while deeper layers align more with global semantics. This suggests that the layers can be viewed as a pool of specialized “experts”. Inspired by the Mixture-of-Experts (MoE) paradigm, we treat each layer as an expert

and propose a dynamic layer selection framework, called TGIF (Text-Guided Inter-layer Fusion). In this framework, a text-guided “router” learns to generate weights to select and fuse the most relevant layer experts for a given task. We explore two architectures for the TGIF router, one with text-only input and other with multimodal input. The model architecture and framework is shown in Fig 2. This design allows adaptive, query-conditioned fusion of depth-wise visual cues, improving both grounding and fine-grained detail understanding.

#### 3.1.1 Text-Guided MLP Router

Our baseline approach uses a lightweight MLP-based router to predict layer importance scores based solely on the textual prompt. This router learns a direct mapping from the question’s semantics to the relevance of different vision layers. Let  $\mathbf{f}_{\text{text}} \in \mathbb{R}^{D_t}$  be the pooled text embedding from the LLM,  $\{\mathbf{F}_l \in \mathbb{R}^{P \times D_v}\}_{l=1}^L$  be the set of patch-level visual features from all  $L$  layers of the vision encoder. The MLP selector first predicts unnormalized logits for each layer:

$$\mathbf{z} = \text{MLP}(\mathbf{f}_{\text{text}}) \in \mathbb{R}^L. \quad (1)$$

These logits are then transformed into a probability distribution using the softmax function to represent the layer weights:

$$\mathbf{w} = \text{softmax}(\mathbf{z}) \in \mathbb{R}^L. \quad (2)$$

The final fused visual representation is computed as a weighted sum of all layer features, where the weights are broadcast across the patch and feature dimensions:

$$\mathbf{F}_{\text{fused}} = \sum_{l=1}^L w_l \cdot \mathbf{F}_l \in \mathbb{R}^{P \times D_v}. \quad (3)$$

#### 3.1.2 Multimodal MLP Router

To address cases in pretraining where the text prompt is generic (e.g., “Describe the image”), we enhance the router with visual context. This multimodal approach allows the selection to be conditioned on both the question and the image content.

We first extract a global image representation,  $\mathbf{f}_{\text{image}} \in \mathbb{R}^{D_v}$ , by taking the [CLS] token from the penultimate layer of the vision encoder. The text and image features are then projected to a common dimension  $D_p$  and concatenated:

$$\mathbf{f}_{\text{multi}} = [\mathbf{f}_{\text{text}} \mathbf{W}_t, \mathbf{f}_{\text{image}} \mathbf{W}_v] \in \mathbb{R}^{2D_p}, \quad (4)$$

where  $\mathbf{W}_t \in \mathbb{R}^{D_t \times D_p}$  and  $\mathbf{W}_v \in \mathbb{R}^{D_v \times D_p}$  are learnable projection matrices. This combined multimodal feature vector is then used by the MLP to predict the layer weights, following the same process as in Equations 1-3. A schematic comparison between the text-only and multimodal routers is provided in Appendix B (Fig. 7).

### 3.2 Load Balancing Loss

A common challenge when training MoE-style routers is the tendency for the router to converge to a state where it consistently selects the same few “safe” experts (in our case, layers), leading to “expert starvation” [33]. To mitigate this and encourage the router to utilize a more diverse set of layers, we incorporate a modified auxiliary load balancing loss into our total training objective.

For our soft-selection routers, we use an entropy-based loss. Let  $w_b \in \mathbb{R}^L$  be the layer weights for the  $b$ -th sample in a batch of size  $B$ . We first compute the average weight for each layer across the batch:

$$\bar{w} = \frac{1}{B} \sum_{b=1}^B w_b \in \mathbb{R}^L. \quad (5)$$

The auxiliary loss is then formulated to maximize the entropy of this average distribution, which encourages a more uniform usage of layers:

$$\mathcal{L}_{\text{aux}} = \lambda \sum_{l=1}^L \bar{w}_l \log(\bar{w}_l + \epsilon), \quad (6)$$

where  $\lambda$  is a hyperparameter controlling the strength of the loss and  $\epsilon$  is a small constant for numerical stability. This auxiliary loss is added to the main VLM loss during training.

Because the nature of textual prompts differs between pre-training and instruction tuning dataset, we apply different  $\lambda$  values across stages. During pretraining, the router often receives generic prompts (e.g., “Describe the image”), which provide limited textual guidance. We thus strengthen the visual signal by applying a slightly larger  $\lambda$  to encourage exploration of multiple layers. During fine-tuning, prompts are task-oriented and semantically rich (e.g., “What number is written on the sign?”). So we reduce  $\lambda$  to allow the router to focus on discriminative, text-conditioned layer selection.

## 4 Experiments

In this section, we present a comprehensive evaluation of our proposed TGIF framework. We compare our best-performing model against the LLaVA-1.5 baseline and then provide a detailed analysis of our ablation studies to understand the contributions of different components of our design.

### 4.1 Experimental Setting

#### 4.1.1 Implementation Details

We implement our proposed framework, TGIF, on top of the publicly available LLaVA-1.5 [17] codebase. To ensure a fair comparison, our primary experiments maintain consistency with LLaVA-1.5 by employing CLIP-ViT-L/14-336px [31] as the vision encoder and Vicuna-7B [8] as the LLM.

#### 4.1.2 Training Recipe

All models are trained on 8 NVIDIA H100-80G GPUs following the two-stage training paradigm of LLaVA-1.5 [17], consisting of **Stage 1: Feature Alignment Pretraining** and **Stage 2: Instruction Finetuning**. For a fair comparison, we adopt the same training datasets and data splits as LLaVA-1.5. Implementation details for each stage are provided in Sec. C. We also apply stage-specific load balancing coefficients (Sec. 3.2) to encourage diverse layer usage during pretraining and more discriminative text-conditioned routing during fine-tuning.

#### 4.1.3 Evaluation Benchmarks

To comprehensively evaluate our TGIF framework, we benchmark its performance across a diverse set of multimodal tasks spanning hallucination detection, fine-grained OCR reasoning, and general visual question answering. All evaluations are conducted using the standardized VLMEvalKit [11] platform to ensure consistency and comparability across models.

**Hallucination Benchmarks.** To assess grounding faithfulness, we adopt two representative hallucination benchmarks: HallusionBench (HB) [22] and POPE [20]. HallusionBench probes visual factuality by testing a model’s ability to reject implausible object claims, while POPE reformulates hallucination detection as a binary classification task, quantifying the model’s awareness of object existence.

**OCR Benchmarks.** To evaluate text recognition and detail-sensitive reasoning, we include TextVQA [34] and the comprehensive OCRBench [29], which covers scene-text, document-text, and key information extraction subtasks. These benchmarks reveal the model’s ability to retrieve and interpret fine-grained textual cues—an area where hallucination often manifests due to overreliance on semantic priors.

**General Reasoning and Overall Benchmarks.** For overall multimodal reasoning performance, we report results on widely used visual QA and instruction-following datasets, including MMBench (MMB) [28], ScienceQA [30] and GQA [2]. Together, these benchmarks measure both the factual grounding and generalization capability of TGIF across visual domains and task types.

#### 4.1.4 Baseline Methods

We evaluate TGIF against two complementary categories of baselines:

**Decoding-based Hallucination Mitigation.** VCD [16], VTI [27], OPERA [14], FarSight [36], and PerturboLLaVA [6] intervene at decoding or inference time without modifying visual representations.

**Multi-layer Fusion Baselines.** DenseConnector [42] and MM-Fuser [5] aggregate features from multiple vision encoder layers using static fusion strategies.

Table 1: **Comparison across VLM benchmarks. Hallucination:** POPE and HallusionBench(HB). **OCR:** TextVQA and OCRBench. **Overall:** ScienceQA(SQA), GQA, MMBench. Best in **bold**, second best underlined. † Our final TGIF model; other TGIF variants explore router design choices.

METHOD	HALLUCINATION		OCR		OVERALL		
	POPE	HB	TEXTVQA	OCRBENCH	SQA	GQA	MMBENCH
<i>Baseline Models</i>							
LLAVA-1.5-7B	86.85	46.27	58.20	30.80	66.80	62.00	64.30
+ DENSECONNECTOR	86.60	–	<b>59.20</b>	–	69.50	<b>63.80</b>	<u>66.80</u>
+ MMFUSER	86.30	–	58.80	–	68.70	<u>62.80</u>	<b>67.50</b>
<i>Proposed Methods (TGIF)</i>							
+ TGIF (TEXT-ONLY ROUTER)	<u>87.30</u>	<u>49.95</u>	58.93	<b>31.50</b>	68.07	62.48	65.97
+ TGIF (MULTIMODAL ROUTER)	86.26	<b>57.31</b>	<u>59.09</u>	29.90	<u>69.72</u>	62.37	65.46
+ <b>TGIF</b> ( $\lambda=0.01$ ) <sup>†</sup>	<b>87.91</b>	48.68	58.98	<u>31.30</u>	<b>70.10</b>	62.58	66.40

Table 2: **POPE comparison.** We report the average F1-score and accuracy averaged across three sub-tasks. Detailed results are provided in the Appendix.

METHOD	ACC $\uparrow$	F1 $\uparrow$
LLAVA-1.5-7B	86.85	85.86
+ VCD	84.66	84.51
+ OPERA	84.20	85.40
+ VTI	86.50	85.90
+ FARSIGHT	86.10	80.40
+ <b>TGIF (OURS)</b>	<b>87.91</b>	<b>86.23</b>

## 4.2 Main Results

Table 1 summarizes TGIF’s quantitative performance across three evaluation families: hallucination, OCR, and general reasoning. Our method consistently improves fine-grained grounding and text perception while maintaining strong overall reasoning ability. Compared to static layer-fusion baselines such as DenseConnector and MMFuser, TGIF’s text-guided routing achieves clear gains on hallucination and OCR benchmarks, validating the effectiveness of adaptive, query-aware fusion. TGIF delivers consistent improvement on hallucination-focused benchmarks (+3.7% on HallusionBench, +1.1% on POPE) and OCR tasks (+0.9% on TextVQA, +0.7% on OCRBench), while matching or surpassing DenseConnector and MMFuser on overall reasoning benchmarks. These results demonstrate that text-guided inter-layer fusion enhances grounding precision without compromising high-level semantics.

We further analyze TGIF’s performance on hallucination mitigation, fine-grained perception, and general reasoning to understand its behavior across tasks. For detailed performance comparisons, we adopt the best-performing configuration, TGIF with a pretraining-only load-balancing coefficient of  $\lambda = 0.01$ .

Table 3: **POPE-Adversarial depth analysis.** Static depth choices exhibit complementary failure modes, while TGIF achieves the best F1-score via text-guided inter-layer fusion.

METHOD	ACC $\uparrow$	PREC $\uparrow$	RECALL $\uparrow$	F1 $\uparrow$
LLAVA	0.851	0.899	0.792	0.852
+EARLY-ONLY	0.804	<b>0.963</b>	0.632	0.763
+MID-ONLY	0.840	0.942	0.725	0.819
+LATE-ONLY	0.837	0.800	<b>0.899</b>	0.847
+UNIFORM	0.838	0.957	0.707	0.813
+ <b>TGIF(OURS)</b>	<b>0.860</b>	0.881	0.832	<b>0.856</b>

Unless otherwise specified, **TGIF** refers to this final configuration ( $\lambda=0.01$ ) throughout all tables and figures.

## 4.3 Hallucination Mitigation

### 4.3.1 POPE and HallusionBench

On POPE (Table 2), TGIF achieves the highest accuracy (87.91%) and F1 score (86.23%), surpassing recent decoding-based methods including VCD, OPERA, VTI, and FarSight. On HallusionBench (Table 4), TGIF attains an All Accuracy of 49.94%, outperforming LLaVA-1.5 by +3.0% and exceeding larger 13B-parameter models. This indicates that TGIF reduces both structured and generative hallucinations by providing richer, query-conditioned visual grounding.

### 4.3.2 Trade-off across visual feature depths

Table 3 analyzes hallucination behavior under different visual abstraction depths on POPE-Adversarial. To isolate the effect of feature depth, we mask the inter-layer fusion weights to construct static variants that expose only early (layers 0–7), middle (8–15), or late (16–23) ViT features, as well as a uniform fusion

Table 4: **HallusionBench comparison.** We compare LLaVA-1.5-7B+TGIF with similarly sized open-source models (7–13B). We report GPT4-assisted All Accuracy. Detailed results are provided in the Appendix.

METHOD	PARAMS	ALL ACC $\uparrow$
LLAVA-1.5	13.0B	46.94
QWEN-VL	9.6B	39.15
OPEN-FLAMINGO	9.0B	38.44
INSTRUCTBLIP	8.2B	45.26
MINIGPT5	8.2B	40.30
MINIGPT4	8.2B	35.78
<hr/>		
LLAVA-1.5	7.0B	46.90
+ VCD	7.0B	46.90
+ OPERA	7.0B	47.10
+ PERTURBOLLAVA	7.0B	47.60
<b>+ TGIF (OURS)</b>	7.0B	<b>49.94</b>

Table 5: **OCRBench comparison.** Recog.:Text Recognition;  $VQA^S$ :Scene Text-centric VQA;  $VQA^D$ :Document-oriented VQA; KIE: Key Information Extraction; HMER:Handwritten Math Expression Recognition.

METHOD	RECOG.	$VQA^S$	$VQA^D$	KIE	HMER	FINAL
LLAVA-1.5-7B	160	117	15	5	0	297
<b>+TGIF (OURS)</b>	<b>162</b>	<b>121</b>	<b>24</b>	<b>6</b>	0	<b>313</b>

over all layers. We also report the original LLaVA baseline, which relies on a single late-layer representation (layer  $-2$ ).

The results reveal a clear depth-dependent trade-off. Early-layer features are conservative, achieving high precision but low recall, indicating missed positives due to insufficient semantic abstraction. Late-layer features achieve high recall but exhibit a strong “Yes” bias, leading to increased hallucination under adversarial co-occurrence prompts. Mid-layer and uniform fusion partially balance these effects but remain suboptimal.

In contrast, TGIF dynamically adapts the exposed visual abstraction level based on the input query, achieving the best overall F1-score. This confirms that no single fixed depth is optimal for hallucination robustness and motivates text-guided inter-layer fusion.

#### 4.4 Fine-grained perception

TGIF strengthens visual-text alignment on text-centric reasoning tasks. As shown in Table 5, TGIF improves the overall OCRBench score by +16 points over LLaVA-1.5-7B, driven by better recognition and document VQA accuracy. The gains mainly stem from TGIF’s ability to emphasize low- to mid-level layers that encode edges, text strokes, and local layout cues—features often overlooked by single-layer connectors. These improvements confirm TGIF’s suitability for dense and detail-sensitive multimodal tasks.

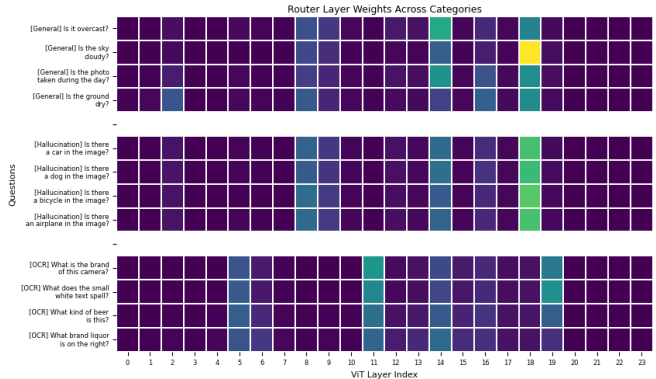


Figure 3: **Router layer selection patterns across different question categories.** This heatmap visualizes the router’s learned weights for selecting vision transformer (ViT) layers across three categories of questions: **General**, **Hallucination Detection**, and **OCR/Detail Recognition**. Each row corresponds to one question, and each column indicates a specific ViT layer. Brighter colors denote higher selection weight for that layer.

#### 4.5 General reasoning

Across general benchmarks (ScienceQA, GQA, MMBench), TGIF maintains competitive reasoning ability. The  $\lambda=0.01$  pretrain-only variant achieves the best ScienceQA accuracy (70.1%) and a strong 66.4% MMBench score, suggesting that dynamic layer fusion generalizes well to unseen instructions. Slight variation in GQA performance is attributed to TGIF’s stronger grounding, which prioritizes factual consistency over speculative generation. Overall, TGIF acts as a grounding-aware regularizer, improving trustworthiness without sacrificing general reasoning.

#### 4.6 Router Layer Selection Dynamics

To understand how TGIF adapts visual fusion to different query types, we visualize the learned layer-weight distributions in Fig. 3. The router exhibits clear, semantically-driven routing patterns. General queries (e.g., “Describe the image.”) activate a broad mixture of mid- and high-level layers, reflecting the need for holistic scene understanding. Hallucination-sensitive queries place greater weight on early layers that preserve spatial and boundary cues, which helps verify object presence rather than relying on language priors. In contrast, OCR and detail-oriented questions concentrate weight on mid-to-late layers containing rich text strokes and structural detail. These behaviors confirm that TGIF does not rely on a fixed mixture but instead performs question-aware selection of visual experts, addressing the limitations of static multi-layer fusion.

#### 4.7 Ablation Studies

We conduct ablation studies to analyze the design choices of TGIF, focusing on (i) the effect of multimodal guidance in the

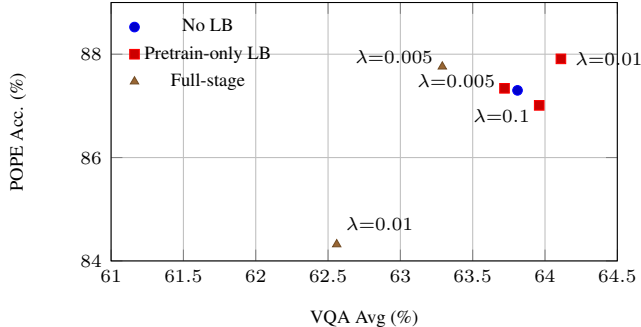


Figure 4: **Effect of load balancing on the VQA–hallucination trade-off.** Each point shows the average VQA score (ScienceQA, GQA, TextVQA) versus POPE accuracy for a different router / load-balancing configuration. We annotate all load-balancing settings next to their corresponding points.

router, and (ii) the role of the entropy-based load-balancing loss.

#### 4.7.1 Text-only vs. Multimodal Routing

We compare two routing strategies: text-only router that conditions solely on the question embedding, and a multimodal router that additionally incorporates a global image representation. As shown in Table 1, both variants consistently outperform the LLaVA-1.5 baseline, confirming the effectiveness of dynamic inter-layer fusion.

The multimodal router achieves a substantial gain on HallusionBench(57.31 vs. 49.95), suggesting that global visual context can help the router better distinguish queries requiring semantic reasoning from those demanding conservative verification. It also improves performance on ScienceQA, indicating stronger generalization on complex, multi-step reasoning tasks.

In contrast, the text-only router performs slightly better on POPE and OCRBench, where hallucination often arises from over-reliance on semantic co-occurrence rather than insufficient visual context. In these cases, conditioning routing solely on the linguistic intent of the query encourages more conservative layer selection, reducing sensitivity to visually plausible but absent objects. This behavior aligns with our hypothesis that hallucination is strongly influenced by how visual abstraction depth is exposed to the language model.

Overall, while multimodal routing can benefit tasks that require global semantic understanding, we adopt the text-only router as our final configuration due to its stronger and more stable performance on hallucination-sensitive and fine-grained perception benchmarks. This choice also better isolates the effect of query-driven control over visual representation depth, which is the central focus of TGIF.

#### 4.7.2 Effect of Load-Balancing Coefficient $\lambda$

We further analyze the impact of the entropy-based load-balancing loss on routing stability and downstream performance. As

Table 6: **Computation and memory overhead.** Parameter count, inference latency, and peak GPU memory usage. TGIF introduces negligible overhead relative to the LLaVA-1.5 baseline.

MODEL	PARAMS (M)	LATENCY (s)	PEAK MEM (GB)
LLAVA	7062.9	0.2203	27.16
+ TGIF	7065.0	0.2224	27.16
OVERHEAD	+0.03%	+0.93%	+0.00

shown in Fig. 4, applying a small amount of regularization during pretraining only provides the best balance between VQA accuracy and hallucination robustness. In particular, the  $\lambda=0.01$  pretrain-only configuration yields both the highest POPE accuracy and the strongest average VQA score, indicating that mild early-stage entropy encourages the router to explore a diverse set of layers without suppressing its ability to specialize.

In contrast, larger coefficients (e.g.,  $\lambda=0.1$ ) or applying the loss throughout full fine-tuning tend to over-regularize the router, pulling the layer distribution toward uniformity and reducing its ability to adapt the fusion pattern to the input query. These settings achieve weaker VQA performance and, in some cases, degraded hallucination resistance. Overall, the results suggest that light, pretraining-only regularization is crucial: it stabilizes routing and prevents expert collapse while still allowing the model to learn query-dependent, discriminative layer selection during instruction tuning.

## 4.8 Computation and Memory Overhead

We analyze the parameter, latency, and memory overhead introduced by TGIF to validate its lightweight design. The minimal runtime overhead is expected for two reasons. First, the router is a shallow MLP evaluated once per input and contributes negligible computation compared to the frozen vision encoder and the large language model. Second, LLaVA already computes and stores intermediate visual features across layers during the forward pass, so TGIF does not introduce additional vision encoder computation or memory allocation. Instead, it reweights existing representations prior to projection.

Overall, these results confirm that TGIF provides dynamic, query-conditioned control over visual abstraction depth while remaining parameter-efficient and inference-efficient, making it suitable for large-scale deployment without compromising throughput or memory constraints.

## 4.9 Qualitative comparison

Figure 5 illustrates how text-guided inter-layer fusion alters the visual evidence exposed to the language model. The adversarial query asks whether a traffic light is present. Although the image contains no traffic light, the baseline LLaVA attends strongly to a centrally located fire hydrant whose color and shape are highly correlated with traffic lights in the training distribution. This over-reliance on late, semantically aligned visual features

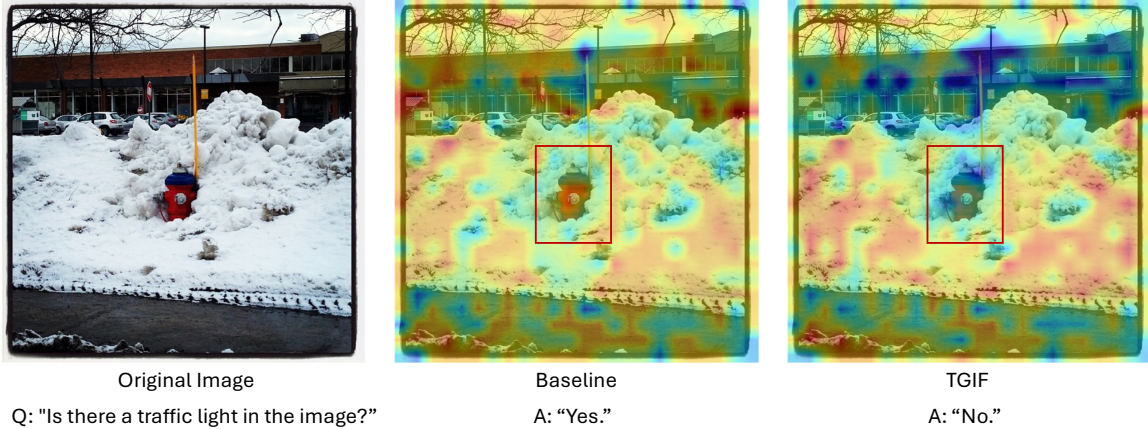


Figure 5: **Qualitative comparison on POPE adversarial.** **Left:** original image. **Middle:** baseline LLaVA text-conditioned relevance map. **Right:** TGIF text-conditioned relevance map. The baseline model attends strongly to a semantically misleading object (a fire hydrant resembling a traffic light), resulting in a hallucinated positive answer. In contrast, TGIF suppresses attention to this spurious region and redistributes relevance toward broader visual evidence, leading to a correct negative response.

leads the model to hallucinate a positive answer.

In contrast, TGIF dynamically reweights visual representations across layers conditioned on the text query. The resulting relevance map deemphasizes the misleading object and distributes attention more broadly across the scene, suppressing language-driven semantic shortcuts. As a result, TGIF correctly answers “No.” While this is a single example, it qualitatively demonstrates how text-guided layer fusion modulates the balance between visual abstraction and language priors, consistent with our quantitative improvements on hallucination benchmarks.

## 5 Conclusion

We presented TGIF, a lightweight text-guided inter-layer fusion framework that dynamically controls which visual representations are exposed to the language model. Our analysis shows that hallucination in multimodal LLMs is closely tied to the depth of visual features used for reasoning, with shallow and deep layers exhibiting complementary failure modes. By adapting the visual abstraction level to the input query, TGIF improves visual grounding and reduces hallucination without modifying the vision encoder, increasing token count, or introducing significant computational overhead. Extensive experiments across hallucination, OCR, and general VQA benchmarks demonstrate that TGIF consistently outperforms strong baselines while preserving overall reasoning capability. These results suggest that query-adaptive control of visual feature depth is a promising direction for building more reliable and trustworthy multimodal language models.

## References

- [1] Gpt-4v(ision) system card. 2023.
- [2] Joshua Ainslie, James Lee-Thorp, Michiel de Jong, Yury Zemlyanskiy, Federico Lebrón, and Sumit Sanghai. Gqa: Training generalized multi-query transformer models from multi-head checkpoints, 2023.
- [3] Jean-Baptiste Alayrac, Jeff Donahue, Pauline Luc, Antoine Miech, Iain Barr, Yana Hasson, Karel Lenc, Arthur Mensch, Katherine Millican, Malcolm Reynolds, et al. Flamingo: a visual language model for few-shot learning. *Advances in Neural Information Processing Systems*, 35:23716–23736, 2022.
- [4] Jinze Bai, Shuai Bai, Shusheng Yang, Shijie Wang, Sinan Tan, Peng Wang, Junyang Lin, Chang Zhou, and Jingren Zhou. Qwen-vl: A frontier large vision-language model with versatile abilities. *ArXiv*, abs/2308.12966, 2023.
- [5] Yue Cao, Yangzhou Liu, Zhe Chen, Guangchen Shi, Wenhai Wang, Danhuai Zhao, and Tong Lu. Mmfuser: Multimodal multi-layer feature fuser for fine-grained vision-language understanding, 2024.
- [6] Cong Chen, Mingyu Liu, Chenchen Jing, Yizhou Zhou, Fengyun Rao, Hao Chen, Bo Zhang, and Chunhua Shen. Perturbollava: Reducing multimodal hallucinations with perturbative visual training, 2025.
- [7] Haoran Chen, Junyan Lin, Xinghao Chen, Yue Fan, Jianfeng Dong, Xin Jin, Hui Su, Jinlan Fu, and Xiaoyu Shen. Multimodal language models see better when they look shallower, 2025.
- [8] Wei-Lin Chiang, Zhuohan Li, Zi Lin, Ying Sheng, Zhanghao Wu, Hao Zhang, Lianmin Zheng, Siyuan Zhuang, Yonghao Zhuang, Joseph E Gonzalez, et al. Vicuna: An

open-source chatbot impressing gpt-4 with 90% chatgpt quality, 2023.

- [9] Wenliang Dai, Junnan Li, Dongxu Li, Anthony Meng Huat Tiong, Junqi Zhao, Weisheng Wang, Boyang Li, Pascale Fung, and Steven Hoi. Instructblip: Towards general-purpose vision-language models with instruction tuning. *arXiv:2305.06500*, 2023.
- [10] Wenliang Dai, Junnan Li, Dongxu Li, Anthony Meng Huat Tiong, Junqi Zhao, Weisheng Wang, Boyang Li, Pascale Fung, and Steven Hoi. Instructblip: Towards general-purpose vision-language models with instruction tuning. *arXiv preprint arXiv:2305.06500*, 2023.
- [11] Haodong Duan, Junming Yang, Yuxuan Qiao, Xinyu Fang, Lin Chen, Yuan Liu, Xiaoyi Dong, Yuhang Zang, Pan Zhang, Jiaqi Wang, et al. Vlmevalkit: An open-source toolkit for evaluating large multi-modality models. In *Proceedings of the 32nd ACM International Conference on Multimedia*, pages 11198–11201, 2024.
- [12] Yossi Gandelsman, Alexei A. Efros, and Jacob Steinhardt. Interpreting clip’s image representation via text-based decomposition, 2024.
- [13] Anisha Gunjal, Jihan Yin, and Erhan Bas. Detecting and preventing hallucinations in large vision language models, 2024.
- [14] Qidong Huang, Xiaoyi Dong, Pan Zhang, Bin Wang, Conghui He, Jiaqi Wang, Dahua Lin, Weiming Zhang, and Nenghai Yu. Opera: Alleviating hallucination in multimodal large language models via over-trust penalty and retrospection-allocation. In *Proceedings of the IEEE/CVF Conference on Computer Vision and Pattern Recognition*, pages 13418–13427, 2024.
- [15] Drew A Hudson and Christopher D Manning. Gqa: A new dataset for real-world visual reasoning and compositional question answering. In *Proceedings of the IEEE/CVF conference on computer vision and pattern recognition*, pages 6700–6709, 2019.
- [16] Sicong Leng, Hang Zhang, Guanzheng Chen, Xin Li, Shijian Lu, Chunyan Miao, and Lidong Bing. Mitigating object hallucinations in large vision-language models through visual contrastive decoding, 2023.
- [17] Chunyuan Li, Cliff Wong, Sheng Zhang, Naoto Usuyama, Haotian Liu, Jianwei Yang, Tristan Naumann, Hoifung Poon, and Jianfeng Gao. Llava-med: Training a large language-and-vision assistant for biomedicine in one day. *arXiv:2306.00890*, 2023.
- [18] Junnan Li, Dongxu Li, Silvio Savarese, and Steven Hoi. Blip-2: Bootstrapping language-image pre-training with frozen image encoders and large language models. *arXiv:2301.12597*, 2023.
- [19] Junnan Li, Dongxu Li, Silvio Savarese, and Steven C. H. Hoi. Blip-2: Bootstrapping language-image pre-training with frozen image encoders and large language models. *ArXiv*, abs/2301.12597, 2023.
- [20] Yifan Li, Yifan Du, Kun Zhou, Jinpeng Wang, Wayne Xin Zhao, and Ji-Rong Wen. Evaluating object hallucination in large vision-language models. In *The 2023 Conference on Empirical Methods in Natural Language Processing*, 2023.
- [21] Junyan Lin, Haoran Chen, Yue Fan, Yingqi Fan, Xin Jin, Hui Su, Jinlan Fu, and Xiaoyu Shen. Multi-layer visual feature fusion in multimodal llms: Methods, analysis, and best practices, 2025.
- [22] Fuxiao Liu, Tianrui Guan, Zongxia Li, Lichang Chen, Yaser Yacoob, Dinesh Manocha, and Tianyi Zhou. Hallusionbench: You see what you think? or you think what you see? an image-context reasoning benchmark challenging for gpt-4v (ision), llava-1.5, and other multi-modality models. In *CVPR*, 2024.
- [23] Fuxiao Liu, Kevin Lin, Linjie Li, Jianfeng Wang, Yaser Yacoob, and Lijuan Wang. Aligning large multi-modal model with robust instruction tuning. *arXiv preprint arXiv:2306.14565*, 2023.
- [24] Hanchao Liu, Wenyuan Xue, Yifei Chen, Dapeng Chen, Xiutian Zhao, Ke Wang, Liping Hou, Rongjun Li, and Wei Peng. A survey on hallucination in large vision-language models, 2024.
- [25] Haotian Liu, Chunyuan Li, Yuheng Li, and Yong Jae Lee. Improved baselines with visual instruction tuning. *arXiv:2310.03744*, 2023.
- [26] Haotian Liu, Chunyuan Li, Qingyang Wu, and Yong Jae Lee. Visual instruction tuning. *arXiv:2304.08485*, 2023.
- [27] Sheng Liu, Haotian Ye, Lei Xing, and James Zou. Reducing hallucinations in vision-language models via latent space steering, 2024.
- [28] Yuan Liu, Haodong Duan, Yuanhan Zhang, Bo Li, Songyang Zhang, Wangbo Zhao, Yike Yuan, Jiaqi Wang, Conghui He, Ziwei Liu, et al. Mmbench: Is your multimodal model an all-around player? In *European conference on computer vision*, pages 216–233. Springer, 2024.
- [29] Yuliang Liu, Zhang Li, Mingxin Huang, Biao Yang, Wenwen Yu, Chunyuan Li, Xu-Cheng Yin, Cheng-Lin Liu, Lianwen Jin, and Xiang Bai. Ocrbench: on the hidden mystery of ocr in large multimodal models. *Science China Information Sciences*, 67(12), December 2024.
- [30] Pan Lu, Swaroop Mishra, Tony Xia, Liang Qiu, Kai-Wei Chang, Song-Chun Zhu, Oyvind Tafjord, Peter Clark, and Ashwin Kalyan. Learn to explain: Multimodal reasoning

- via thought chains for science question answering. In *The 36th Conference on Neural Information Processing Systems (NeurIPS)*, 2022.
- [31] Alec Radford, Jong Wook Kim, Chris Hallacy, Aditya Ramesh, Gabriel Goh, Sandhini Agarwal, Girish Sastry, Amanda Askell, Pamela Mishkin, Jack Clark, et al. Learning transferable visual models from natural language supervision. In *ICML*, 2021.
- [32] Anna Rohrbach, Lisa Anne Hendricks, Kaylee Burns, Trevor Darrell, and Kate Saenko. Object hallucination in image captioning, 2019.
- [33] Noam Shazeer, Azalia Mirhoseini, Krzysztof Maziarz, Andy Davis, Quoc Le, Geoffrey Hinton, and Jeff Dean. Outrageously large neural networks: The sparsely-gated mixture-of-experts layer, 2017.
- [34] Amanpreet Singh, Vivek Natarajan, Meet Shah, Yu Jiang, Xinlei Chen, Dhruv Batra, Devi Parikh, and Marcus Rohrbach. Towards vqa models that can read, 2019.
- [35] Amanpreet Singh, Vivek Natarajan, Meet Shah, Yu Jiang, Xinlei Chen, Dhruv Batra, Devi Parikh, and Marcus Rohrbach. Towards vqa models that can read. In *Proceedings of the IEEE/CVF Conference on Computer Vision and Pattern Recognition (CVPR)*, June 2019.
- [36] Feilong Tang, Chengzhi Liu, Zhongxing Xu, Ming Hu, Zelin Peng, Zhiwei Yang, Jionglong Su, Minquan Lin, Yifan Peng, Xuelian Cheng, Imran Razzak, and Zongyuan Ge. Seeing far and clearly: Mitigating hallucinations in mllms with attention causal decoding, 2025.
- [37] Anthropic Team. Claude 3, 2024.
- [38] Gemini Team. Gemini: A family of highly capable multi-modal models, 2023.
- [39] Bingkui Tong, Jiaer Xia, and Kaiyang Zhou. Mitigating hallucination in multimodal llms with layer contrastive decoding, 2025.
- [40] Jianfeng Wang, Zhengyuan Yang, Xiaowei Hu, Linjie Li, Kevin Lin, Zhe Gan, Zicheng Liu, Ce Liu, and Lijuan Wang. Git: A generative image-to-text transformer for vision and language. *ArXiv*, abs/2205.14100, 2022.
- [41] Jiaqi Wang, Yifei Gao, and Jitao Sang. Valid: Mitigating the hallucination of large vision language models by visual layer fusion contrastive decoding, 2025.
- [42] Huanjin Yao, Wenhao Wu, Taojiannan Yang, YuXin Song, Mengxi Zhang, Haocheng Feng, Yifan Sun, Zhiheng Li, Wanli Ouyang, and Jingdong Wang. Dense connector for mllms, 2024.
- [43] Jiabo Ye, Anwen Hu, Haiyang Xu, Qinghao Ye, Ming Yan, Yuhao Dan, Chenlin Zhao, Guohai Xu, Chenliang Li, Junfeng Tian, et al. mplug-docowl: Modularized multi-modal large language model for document understanding. *arXiv:2307.02499*, 2023.
- [44] Qinghao Ye, Haiyang Xu, Guohai Xu, Jiabo Ye, Ming Yan, Yiyang Zhou, Junyang Wang, Anwen Hu, Pengcheng Shi, Yaya Shi, et al. mplug-owl: Modularization empowers large language models with multimodality. *arXiv:2304.14178*, 2023.
- [45] Qinghao Ye, Haiyang Xu, Jiabo Ye, Ming Yan, Anwen Hu, Haowei Liu, Qi Qian, Ji Zhang, Fei Huang, and Jingren Zhou. mplug-owl2: Revolutionizing multi-modal large language model with modality collaboration, 2023.
- [46] Tianyu Yu, Yuan Yao, Haoye Zhang, Taiwen He, Yifeng Han, Ganqu Cui, Jinyi Hu, Zhiyuan Liu, Hai-Tao Zheng, Maosong Sun, and Tat-Seng Chua. Rlhf-v: Towards trustworthy mllms via behavior alignment from fine-grained correctional human feedback, 2024.
- [47] Yanzhe Zhang, Ruiyi Zhang, Jiuxiang Gu, Yufan Zhou, Nedim Lipka, Diyi Yang, and Tongfei Sun. Llavar: Enhanced visual instruction tuning for text-rich image understanding. *ArXiv*, abs/2306.17107, 2023.
- [48] Kaizhi Zheng, Xuehai He, and Xin Eric Wang. Minigt-5: Interleaved vision-and-language generation via generative vokens. *ArXiv*, abs/2310.02239, 2023.
- [49] Deyao Zhu, Jun Chen, Xiaoqian Shen, Xiang Li, and Mohamed Elhoseiny. Minigt-4: Enhancing vision-language understanding with advanced large language models. *arXiv preprint arXiv:2304.10592*, 2023.
- [50] Deyao Zhu, Jun Chen, Xiaoqian Shen, Xiang Li, and Mohamed Elhoseiny. Minigt-4: Enhancing vision-language understanding with advanced large language models. *arXiv:2304.10592*, 2023.

## A Architectural Comparison with Prior Layer Fusion Designs

Figure 6 provides a schematic comparison between commonly used multimodal connectors and the proposed text-guided inter-layer fusion (TGIF).

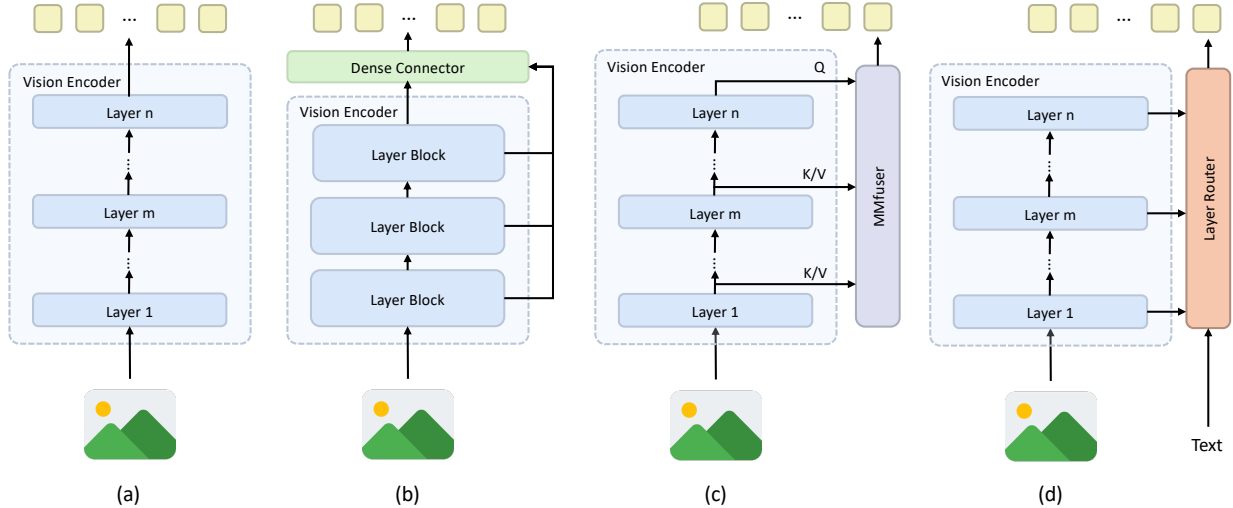


Figure 6: **Comparison of layer fusion designs in MLLMs.** (a) **MLP Connector**: Projects visual tokens from a single, fixed (typically penultimate) vision encoder layer. (b) **Dense Connector**: Aggregates features from multiple layers via concatenation or downsampling with a static fusion pattern. (c) **MMFuser**: Retrieves shallow-layer features using deep-layer queries through cross-attention to recover local details. (d) **TGIF (ours)**: Introduces a text-guided router that dynamically reweights visual features across layers based on the input query, enabling adaptive control over visual abstraction depth.

**Single-layer projection.** Most existing MLLMs, including LLaVA-style architectures, employ a simple MLP connector that projects visual tokens from a single, fixed layer of the vision encoder (typically the penultimate layer) into the LLM. While computationally efficient, this design exposes only late-stage semantic representations to the language model, limiting access to low-level and mid-level visual evidence that is often crucial for fine-grained grounding and hallucination verification.

**Static multi-layer fusion.** Recent works enrich visual representations by aggregating features from multiple encoder layers. DenseConnector concatenates or downsamples features from selected depths, while MMFuser retrieves shallow-layer details using deep-layer queries via cross-attention. Although these approaches improve visual richness, the fusion strategy remains *static*: the set of layers and their relative contributions are fixed once chosen and do not adapt to the input query.

**Text-guided inter-layer fusion (TGIF).** In contrast, TGIF treats the layers of a frozen vision encoder as a pool of specialized visual experts and dynamically selects among them conditioned on the input text. A lightweight router predicts a soft distribution over layers for each query, allowing the model to adaptively control which level of visual abstraction is exposed to the LLM. This enables conservative, low-level verification for hallucination-sensitive queries and higher-level semantic aggregation for descriptive or reasoning-oriented prompts.

Overall, this comparison highlights a key distinction between TGIF and prior fusion methods: rather than statically enriching visual representations, TGIF introduces query-dependent control over visual abstraction depth, directly addressing hallucination arising from mismatched visual evidence.

## B Router Variants: Text-only vs. Multimodal

Figure 7 illustrates the difference between the two routing variants used in TGIF. The **text-only router** predicts layer weights solely from the question embedding, while the **multimodal router** additionally incorporates a global image representation (the penultimate-layer [CLS] token), enabling routing to depend on both query intent and coarse image content.

## C Implementation Details

**Hardware & Precision.** All experiments are conducted on a single node equipped with  $8 \times$  NVIDIA H100 (80GB) GPUs. We utilize DeepSpeed ZeRO (Stage 2 for pretraining, Stage 3 for instruction tuning) to optimize memory efficiency. Unless

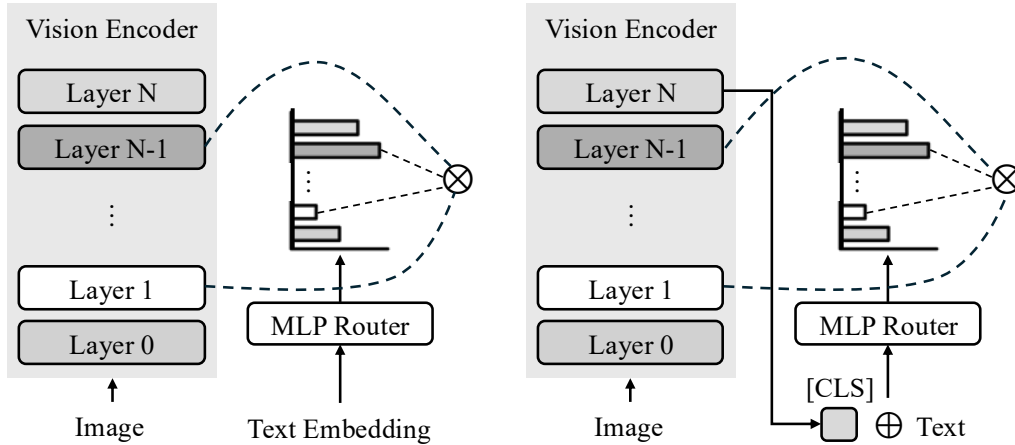


Figure 7: **Text-only vs. multimodal router in TGIF.** **Left:** The text-only router takes the question embedding  $\mathbf{f}_{\text{ext}}$  and outputs layer weights  $w_{\text{layer}}$  via an MLP and softmax. **Right:** The multimodal router concatenates a projected text embedding  $\mathbf{f}_{\text{ext}}\mathbf{W}_t$  and a projected global image embedding  $\mathbf{f}_{\text{image}}\mathbf{W}_v$  (penultimate-layer [CLS]) to form  $\mathbf{f}_{\text{multi}} \in \mathbb{R}^{2D_p}$  before predicting  $w_{\text{layer}}$ .

otherwise specified, we employ Vicuna-7B-v1.5 as the language model and CLIP ViT-L/14@336px as the frozen vision encoder. Training is performed with `bf16` precision and `tf32` matrix multiplication acceleration.

**Stage 1: Feature Alignment.** Following the LLaVA-1.5 protocol, we train only the multimodal projector (including the proposed TGIF router) for 1 epoch on the LLaVA pretraining dataset (558K image–text pairs). We utilize a learning rate of  $1 \times 10^{-3}$  with a cosine decay schedule and a warmup ratio of 0.03. The global batch size is set to 32 (gradient accumulation steps = 1), with a maximum sequence length of 2048. Weight decay is set to 0.

**Stage 2: Instruction Tuning.** In the second stage, we fine-tune the projector and the LLM on the LLaVA v1.5 mixture (665K samples) for 1 epoch. We reduce the learning rate to  $2 \times 10^{-5}$  while maintaining the cosine schedule, warmup ratio of 0.03, and weight decay of 0. The per-GPU batch size is adjusted to 16.

Throughout both stages, the vision encoder remains entirely frozen. We enable gradient checkpointing to conserve memory. All specific hyperparameters and script templates are provided in the attached code for reproducibility.

## D Benchmark Descriptions

### D.1 Hallucination Evaluation

**POPE [20].** POPE assesses object hallucination via a binary verification task. For a given image, the model must answer Yes/No questions (e.g., “Is there a <object> in the image?”). Negative samples are generated using three strategies: (1) **Random** sampling, (2) **Popular** COCO categories, and (3) **Adversarial** co-occurring objects. This setup isolates visual grounding capabilities from captioning priors. We report Accuracy, Precision, Recall, F1-score, and the “Yes” response ratio.

**HallusionBench [22]** This benchmark evaluates visual factual grounding by presenting questions with fabricated or contradictory premises. Unlike standard VQA, HallusionBench penalizes models for failing to reject incorrect visual claims regarding object existence, attributes, and spatial relations. Following the official protocol, we employ a GPT-4 assisted evaluation metric. We report **aAcc** (All Accuracy) as the primary metric, alongside **qAcc** (Question-Pair Accuracy) and **fAcc** (Figure Accuracy).

### D.2 OCR Evaluation

**OCRBench [29].** OCRBench is a comprehensive evaluation suite consisting of 1,000 manually verified QA pairs aggregated from 29 diverse datasets. It assesses five core capabilities: Text Recognition, Scene Text VQA, Document VQA, Key Information Extraction (KIE), and Handwritten Math Expression Recognition (HMER). Evaluation is performed via exact string matching.

**TextVQA [35].** TextVQA is a benchmark designed to evaluate a model’s ability to read and reason about text embedded in natural images. It contains over 45K questions paired with images rich in scene text (e.g., signs, posters, menus), where answering explicitly requires OCR and text-based reasoning. The dataset features a highly diverse, open-ended answer space, making it a challenging testbed for fine-grained visual grounding and text-centric multimodal understanding.

### D.3 General Reasoning and Overall Benchmarks.

**ScienceQA [30].** ScienceQA is a large-scale multimodal multiple-choice benchmark designed to evaluate multi-hop scientific reasoning across vision and language. It contains over 21K questions drawn from elementary and high school science curricula, spanning natural, social, and language sciences. Nearly half of the questions include visual context, and most are annotated with grounded lectures and detailed explanations, enabling analysis of both answer accuracy and reasoning quality. ScienceQA is widely used to assess general multimodal reasoning and instruction-following capabilities beyond surface-level perception.

**GQA [15].** GQA is a large-scale visual question answering benchmark designed to evaluate compositional and multi-step visual reasoning. It contains over 22M questions grounded in real-world images, each paired with a scene graph encoding objects, attributes, and relations. Questions are generated to require explicit reasoning over these structured representations, reducing language priors and dataset bias. In addition to accuracy, GQA provides fine-grained metrics to assess consistency and plausibility, making it a standard benchmark for general visual reasoning and scene understanding.

**MMBench [28]** MMBench is a large-scale, fine-grained benchmark designed to systematically evaluate the perceptual and reasoning abilities of vision–language models. It contains 2,974 multiple-choice questions spanning 20 ability dimensions, organized into a three-level taxonomy covering coarse perception, fine-grained perception, and multimodal reasoning. Instead of task-specific evaluation, MMBench assesses models across diverse capability dimensions, providing more diagnostic feedback. To ensure robust and reproducible evaluation, model outputs are matched to answer choices using an LLM-based evaluator, enabling reliable comparison across open-ended generation models.

## E Additional Quantitative Results

### E.1 POPE Breakdown

In Table 7, we provide a detailed breakdown of performance across the Random, Popular, and Adversarial splits of the POPE benchmark. Our method (TGIF) consistently improves Precision and Accuracy across all subsets compared to the LLaVA-1.5 baseline, indicating robust resistance to hallucination regardless of the negative sampling strategy.

Table 7: **POPE results by subset.** Comparison of LLaVA-1.5-7B and LLaVA-1.5-7B+TGIF across different hallucination settings. Best results within each subset are shown in **bold**.

SUBSET	METHOD	F1	ACC	PREC	REC	YES (%)
RANDOM	LLAVA-1.5	0.873	0.882	0.975	0.791	41.9
	<b>+ TGIF</b>	<b>0.891</b>	<b>0.895</b>	0.960	<b>0.831</b>	44.6
POPULAR	LLAVA-1.5	0.861	0.872	0.944	0.791	41.9
	<b>+ TGIF</b>	<b>0.876</b>	<b>0.882</b>	<b>0.926</b>	<b>0.831</b>	44.9
ADVERSARIAL	LLAVA-1.5	0.842	0.851	0.899	0.791	44.0
	<b>+ TGIF</b>	<b>0.856</b>	<b>0.860</b>	<b>0.882</b>	<b>0.831</b>	47.1

### E.2 HallusionBench Leaderboard

Table 8 presents the full HallusionBench correctness leaderboard. TGIF achieves competitive performance among 7B parameters models, particularly in the aAcc metric, surpassing the LLaVA-1.5 baseline and approaching the performance of proprietary models like Gemini Pro Vision.

Notably, despite utilizing a significantly smaller language backbone (7B parameters), TGIF (49.94%) outperforms several larger open-source baselines, including the 13B-parameter LLaVA-1.5 (46.94%) and the 12.1B-parameter BLIP2-T5

Table 8: **HallusionBench correctness leaderboard.** We report Question-pair Accuracy ( $qAcc$ ), Figure Accuracy ( $fAcc$ ), and All Accuracy ( $aAcc$ ). Top-3 models under GPT-4–assisted evaluation are highlighted in **bold**.

METHOD	PARAMS	EVAL	QACC $\uparrow$	FACC $\uparrow$	AACC $\uparrow$
GPT-4V [1]	–	HUMAN	31.42	44.22	67.58
		GPT-4	<b>28.79</b>	<b>39.88</b>	<b>65.28</b>
LLAVA-1.5 [25]	13B	HUMAN	9.45	25.43	47.12
		GPT-4	10.55	<b>24.86</b>	46.94
CLAUDE 3 [37]	–	GPT-4	<b>21.76</b>	<b>28.61</b>	<b>56.86</b>
GEMINI PRO VISION [38]	–	GPT-4	7.69	8.67	36.85
BLIP2-T5 [19]	12.1B	GPT-4	15.16	20.52	48.09
QWEN-VL [4]	9.6B	GPT-4	5.93	6.65	39.15
OPEN-FLAMINGO [3]	9B	GPT-4	6.37	11.27	38.44
MINIGPT-5 [48]	8.2B	GPT-4	10.55	9.83	40.30
MINIGPT-4 [49]	8.2B	GPT-4	8.79	10.12	35.78
INSTRUCTBLIP [10]	8.2B	GPT-4	9.45	10.11	45.26
BLIP-2 [19]	8.2B	GPT-4	5.05	12.43	40.48
MPLUG-OWL v2 [45]	8.2B	GPT-4	13.85	19.94	47.30
MPLUG-OWL v1 [43]	7.2B	GPT-4	9.45	10.40	43.93
LRV-INSTRUCTION [23]	7.2B	GPT-4	8.79	13.01	42.78
<b>LLAVA-1.5 + TGIF (OURS)</b>	7B	GPT-4	<b>17.36</b>	23.70	<b>49.94</b>
GIT [40]	0.8B	GPT-4	5.27	6.36	34.37
RANDOM CHANCE	–	GPT-4	15.60	18.21	45.96

(48.09%) [25, 19]. It secures the third rank overall, trailing only the closed-source models GPT-4V and Claude 3 [1, 37]. This result shows the efficiency of our text-guided fusion strategy: by dynamically routing to the most relevant visual features, TGIF extracts rich grounding signals from the frozen encoder, effectively mitigating hallucination even against models with nearly double the parameter count.

### E.3 OCRBench Performance

We report detailed OCRBench scores in Table 9. TGIF demonstrates improvements in Scene Text VQA ( $VQA^S$ ) and Document VQA ( $VQA^D$ ), contributing to a higher final score compared to the LLaVA-1.5 baseline. This suggests that layer fusion effectively captures fine-grained textual details often lost in single-layer embeddings.

Table 9: **Detailed results on OCRBench.** Breakdown by sub-task: Text Recognition (Recog.), Scene Text VQA ( $VQA^S$ ), Document VQA ( $VQA^D$ ), Key Information Extraction (KIE), and Handwritten Math Expression Recognition (HMER). Best results are shown in **bold**.

METHOD	RECOG.	$VQA^S$	$VQA^D$	KIE	HMER	TOTAL
GEMINI PRO [38]	<b>215</b>	<b>174</b>	128	134	8	<b>659</b>
GPT-4V [1]	167	163	<b>146</b>	<b>160</b>	<b>9</b>	645
MPLUG-Owl2 [45]	153	153	41	19	0	366
LLAVAR [47]	186	122	25	13	0	346
LLAVA-1.5-13B [25]	176	129	19	7	0	331
LLAVA-1.5-7B [25]	160	117	15	5	0	297
<b>+TGIF (OURS)</b>	162	121	24	6	0	313
MPLUG-Owl [44]	172	104	18	3	0	297
INSTRUCTBLIP [9]	168	93	14	1	0	276
BLIP-2 [19]	154	71	10	0	0	235
MINIGPT-4 v2 [50]	124	29	4	0	0	157